325

MASTER

ORNL-3089
UC-34 – Physics
TID-4500 (17th ed.)

PROTON RECOIL ENERGY LOSS DISTRIBUTION IN PLANE GEOMETRY

H. B. Eldridge
P. R. Flusser
R. H. Ritchie

OAK RIDGE NATIONAL LABORATORY
operated by
UNION CARBIDE CORPORATION
for the
U.S. ATOMIC ENERGY COMMISSION

DISCLAIMER

Printed in USA. Price $0.75. Available from the

Office of Technical Services
U. S. Department of Commerce
Washington 25, D. C.

ORNL-3089

Contract No. W-7405-eng-26

HEALTH PHYSICS DIVISION

PROTON RECOIL ENERGY LOSS DISTRIBUTION IN PLANE GEOMETRY

H. B. Eldridge, P. R. Flusser, and R. H. Ritchie

Date Issued

JUL 10 1962

Oak Ridge National Laboratory
Oak Ridge, Tennessee
operated by
Union Carbide Corporation
for the
U. S. Atomic Energy Commission

TABLE OF CONTENTS

PROTON RECOIL ENERGY LOSS DISTRIBUTION IN PLANE GEOMETRY

Abstract

Computations of proton recoil energy losses from neutron irradiation of hydrogenous systems possessing plane symmetry have been made for the purpose of fast neutron counter design. A digital computer code has been written to carry out the calculations for two irradiation geometries: 1) the neutron beam is assumed to be normally incident upon the system, and 2) the system is exposed to an isotropic flux of neutrons. Numerical results are presented for neutrons of various energies incident on plane radiators of different thicknesses for these two irradiation geometries. These results have been used in the conceptual design of fast neutron dosimeters employing a generalized dosimetry principle. The applications are described more fully elsewhere.

I. Introduction

In the design of counters sensitive to proton recoils from fast neutron irradiation, it is of some interest to consider systems possessing plane symmetry. Figure 1 shows the geometry assumed for this problem. Fast neutrons incident on the system, which is assumed to contain hydrogen in the detector and/or wall materials, generate recoil protons throughout. These protons deposit various amounts of their energy in the detector volume, depending upon the distance of the point of their origin from the wall surface F and upon the amounts of energy imparted to them by incident neutrons.

The information required here is the integral recoil distribution, i.e., the number of recoils depositing energy greater than ϵ in the detector volume as a function of neutron energy E. Theoretical information on this function is of importance in adapting plane counting systems for use as fast neutron dosimeters according to a generalized dosimetry principle.[1]

In the past, computations of this quantity have been carried out for certain plane geometries assuming irradiation by a normally incident beam of fast neutrons[2] in order to design a fast neutron counter with a first collision dose response. It may be shown[3] that the isotropic irradiation of a composite plane slab is equivalent to plane irradiation of a spherical shell of the same composition if the radius of the shell is much greater than the maximum range of the most energetic protons. Therefore, similar computations for isotropic irradiation have been made in order to obtain a non-directional response. In addition, calculations of the energy loss under the bias in dosimeters of the Hurst integrating type have been made using the plane parallel model.[4,5]

The present report presents some results of calculations with a digital computer code which has been written for the purpose of calculating the integral recoil distribution function,

$$\int_{\epsilon}^{\infty} d\epsilon' \; n(\epsilon', E)$$

for plane geometries in more detail than has been done previously. Here $n(\epsilon, E)d\epsilon$ is defined to be the number of recoils which deposit energy between ϵ and $\epsilon + d\epsilon$ in the detector volume for a specified material configuration by neutrons of energy E in a given irradiation geometry. The code is designed so that one may obtain an arbitrary moment,

$$I_m(\epsilon, E) \equiv \int_{\epsilon}^{\infty} (\epsilon')^m \, n(\epsilon', E) d\epsilon'$$

of the distribution function.

The method of computation and the input data are given below and a number of graphical representations of

$$\int_{\epsilon}^{E} n(\epsilon', E) d\epsilon'$$

are presented for various geometrical configurations.

II. Method of Computation

In Fig. 1 the breadth of the beam and the lateral extension of the slab are both supposed to be much greater than the range of the most energetic proton which may be generated by an (n-p) reaction in the system. Attenuation of the neutron beam in the system was neglected in the present study. Recoils other than those from the H(n,p) scattering process are also neglected.

One assumes here that if one expresses $R(E_p)$, the range of a recoil proton of energy E_p, in units of gm/cm^2, it will be independent of position in the system. This assumption is not very restrictive in a practical sense. It is well known that the stopping power of a given atom, expressed in terms of energy loss per gm/cm^2, is a slowly varying function of the atomic number Z of that atom. Hence, if one wishes to design a plane system having a given response function for neutrons of a given energy, one may use alternate layers of hydrogenous and non-hydrogenous material in order to obtain the desired response. It is easy to find low Z substances not containing hydrogen which have nearly the same $R(E_p)$ relation as most hydrogenous substances.[2]

In all of the computations described below, it has been assumed that $R(E_p)$ is given by the range-energy relation of protons in a hydrocarbon having the composition $(CH_2)_n$.

If unit flux of neutrons having energy E is incident normally upon the slab under consideration, there will be generated in an incremental thickness dx a number of proton recoils d^2N_p lying in the interval between μ and $\mu + d\mu$ given by

$$d^2N_p = 2\,AN_o\sigma_H(E)\ \mu d\mu\ dx$$

where μ is the cosine of the angle at which a recoil proton emerges from an n-p collision relative to the initial neutron direction, A is the area of the system normal to the beam direction, N_o is the number of hydrogen atoms per unit volume at x and $\sigma_H(E)$ is the n-p cross section at energy E.

The number of these recoils which deposit energy in $d\epsilon$ at ϵ in the detector region is a function of E, x, μ, and the thickness of the detector. This leads to the expression

$$I_m(\epsilon,\ E) = \int_{\epsilon}^{E} (\epsilon')^m\ n_p(\epsilon',\ E)d\epsilon' = 2AN_o\sigma_H(E)\ ' \int_{\mu_1(\epsilon,E)}^{\mu_2(\epsilon,E)} \mu\ d\mu \int_{x_1(\epsilon,E,\mu)}^{x_2(\epsilon,E,\mu)} [\epsilon'\ (x,\mu)]^m$$

where the limits on the μ and x integrations depend upon the range-energy relations of recoil protons in the materials of the system and where the dependence on the detector thickness is not indicated in order to simplify notation. If, however, unit flux of neutrons having energy E is incident isotropically upon a slab, there will be generated in a layer of thickness dx a number of proton recoils d^3N_I lying in the interval between μ and $\mu + d\mu$, ϵ and $\epsilon + d\epsilon$ given by:

$$d^3N_I = N_o A\sigma_H(E) dx \, d\mu \, \frac{d\epsilon}{E}$$

where the symbols have the same meaning as in the normal irradiation case. In this case,

$$I_m^I(\epsilon,E) = \int_\epsilon^E (\epsilon')^m \, n_I(\epsilon',E) d\epsilon' = \frac{N_o \, A\sigma_H(E)}{E} \int_{x_1(\epsilon)}^{x_2(\epsilon)} dx \int_{\mu_1(\epsilon)}^{\mu_2(\epsilon)} d\mu \int_\epsilon^E d\epsilon' (\epsilon')^m$$

The integral energy distribution,

$$I_o(\epsilon,E) = \int_\epsilon^\infty n(\epsilon',E) d\epsilon'$$

was evaluated for a variety of detector and radiator thicknesses (hereafter called gas and wall, respectively) for both normal and isotropic irradiation, utilizing a digital computer. The indicated integrations were carried out using rather standard numerical methods. The integration meshes were chosen as small as possible, commensurate with reasonable computation times. The curves drawn in Figs. 2 through 18 are believed to be accurate to better than ± 3% in most cases.

The range energy relation of protons in $(CH_2)_n$ was taken from the numerical work of Herschfelder and Magee.[6] A table of 59 values of range vs energy was stored in the fast memory, and linear interpolation was used for immediate values (see Table I). In the calculations which have been carried out, the thickness of wall and detector and the range of protons of various energies have all been expressed in mg/cm^2 of material. For the purposes of this computation, the hydrogen cross section was represented by the theoretical equation[7]

$$\sigma_H(E) = \frac{\pi}{1.206\ E + (0.422 - 0.1447\ E)^2} + \frac{3\pi}{(1.206\ E + 5.383)\,[0.6506 + 0.007225\,(1.206\ E + 5.383)]}$$

where σ_H is in units of barns and E is in units of Mev.

The results are presented for the case of normal irradiation in Figs. 2 through 8 where each curve is labeled with the incident neutron energy, and the thickness of gas or wall is expressed in terms of the energy of a proton whose residual range is equal to that thickness. A wall thickness designated as infinite corresponds to a thickness greater than the range of the most energetic recoil proton from an n-p reaction for a given neutron energy. The units of the integral distributions,

$$\int^{E} d\epsilon'\ n(\epsilon', E)$$

for all curves shown are (barn) · $(mg)/cm^2$. In order to obtain the number

Table I. Range-Energy Relation in Paraffin $[(CH_2)_n]$ Taken from Ref. 6

E(Mev)	R(mg/cm^2)	E(Mev)	R(mg/cm^2)
0.0	0.0	2.0	6.268
0.002	0.014	2.1	6.817
0.005	0.02322	2.2	7.385
0.010	0.03197	2.3	7.974
0.015	0.03732	2.4	8.583
0.02	0.04143	2.5	9.212
0.03	0.04824	2.6	9.861
0.04	0.05462	2.7	10.529
0.05	0.06096	2.8	11.217
0.07	0.07350	2.9	11.925
0.10	0.09613	3.0	12.652
0.15	0.1386	3.5	16.571
0.20	0.1891	4.0	20.960
0.30	0.3137	4.5	25.811
0.40	0.4683	5.0	31.118
0.50	0.6512	5.5	36.87
0.6	0.8610	6.0	43.07
0.7	1.0968	6.5	49.70
0.8	1.3576	7.0	56.77
0.9	1.6429	7.5	64.26
1.0	1.9520	8.0	72.18
1.1	2.2845	8.5	80.52
1.2	2.6398	9.0	89.28
1.3	3.0176	10.0	108.02
1.4	3.4175	11.0	128.40
1.5	3.8393	12.0	150.40
1.6	4.2827	13.0	174.00
1.7	4.7476	14.0	199.17
1.8	5.2336	15.0	225.91
1.9	5.7406		

of recoils depositing energy $\geq \epsilon$ in the detector for unit flux incident on a system of area A, atomic hydrogen density N_o and density ρ, one needs only to multiply the ordinates of all curves by $10^{-24} AN_o/\rho$. In order to convert the wall thickness expressed in units of energy to units of length, one must first determine the corresponding range from the range-energy table used and then divide by the density of the material. Figures 9 through 18 show similar results for the case of isotropic irradiation. In all cases considered here it has been assumed that the density of hydrogen, and hence the density of recoils generated, is uniform throughout the system. However, the code is designed so that one may vary the hydrogenic density if desired.

A few calculations were made of $I_1(\epsilon,E)$ and $I_2(\epsilon,E)$, the first and second moment distributions, respectively, of the deposited energy. These have been described in reference 1 and will not be given here. These results have been used in the conceptual design of a fast neutron dosimeter which is assumed to respond to the second moment $I_2(\epsilon,E)$ of the proton distribution.[1] Reference 1 also describes the use of these data, shown in Figs. 1 through 18, in the design of an electronic system which operates on the proton recoil distribution from a simple slab radiator in order to provide a dose-like response with respect to the neutron energy.

UNCLASSIFIED
ORNL-LR-DWG-64841

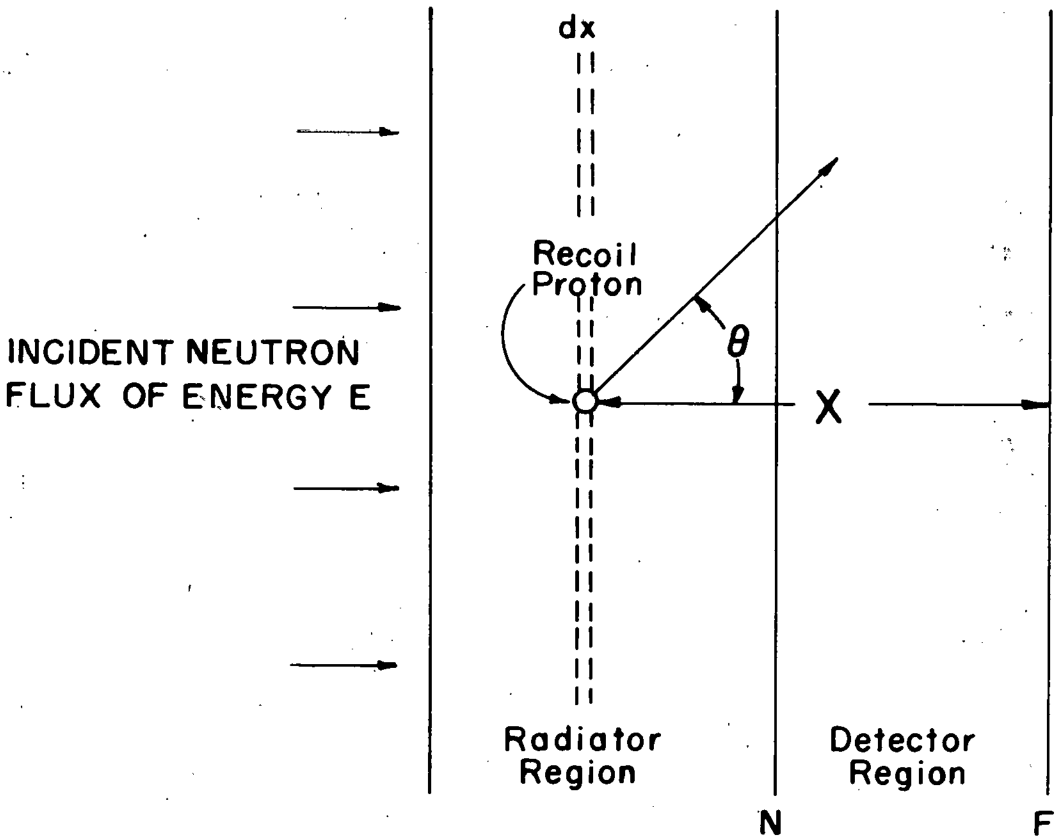

Fig. 1. Schematic Representation of Proton Recoil Counter System.

UNCLASSIFIED
ORNL-LR-DWG. 64609

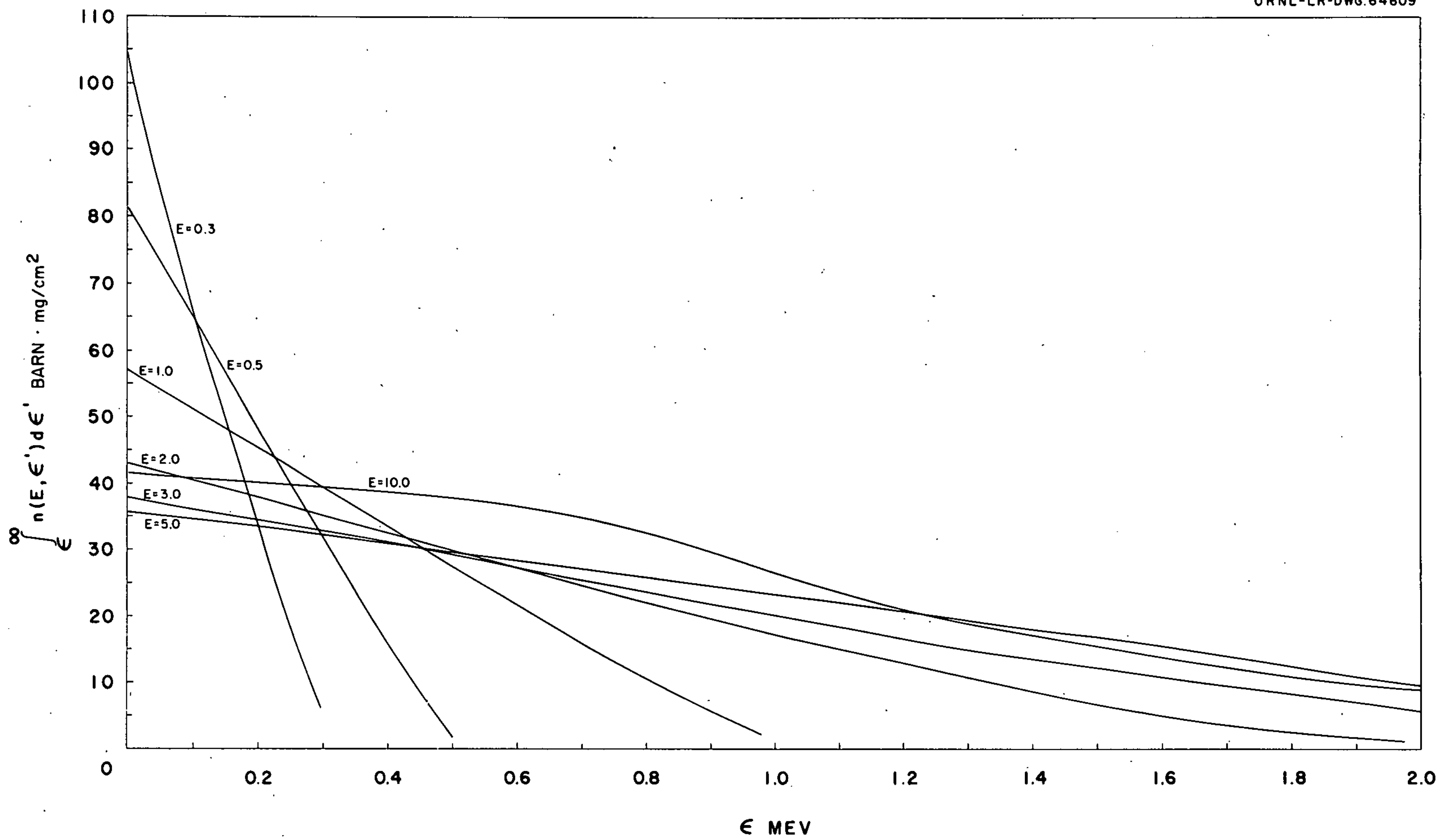

Fig. 2. Integral Response of Plane Detector, Normal Irradiation. (3.0 Mev gas, ∞ wall)

UNCLASSIFIED
ORNL-LR-DWG. 64610

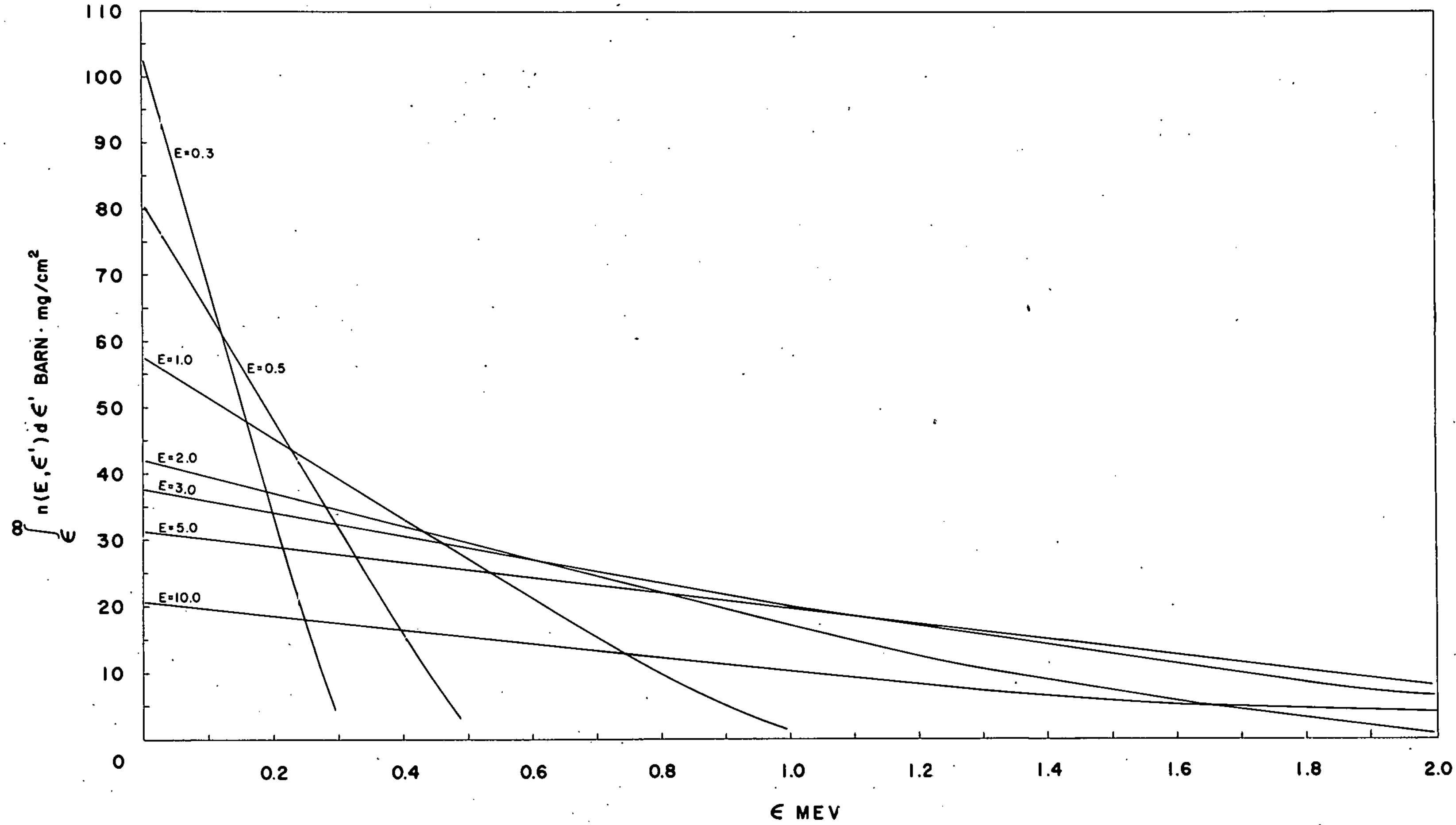

Fig. 3. Integral Response of Plane Detector, Normal Irradiation. (3.0 Mev gas, 3.0 Mev wall)

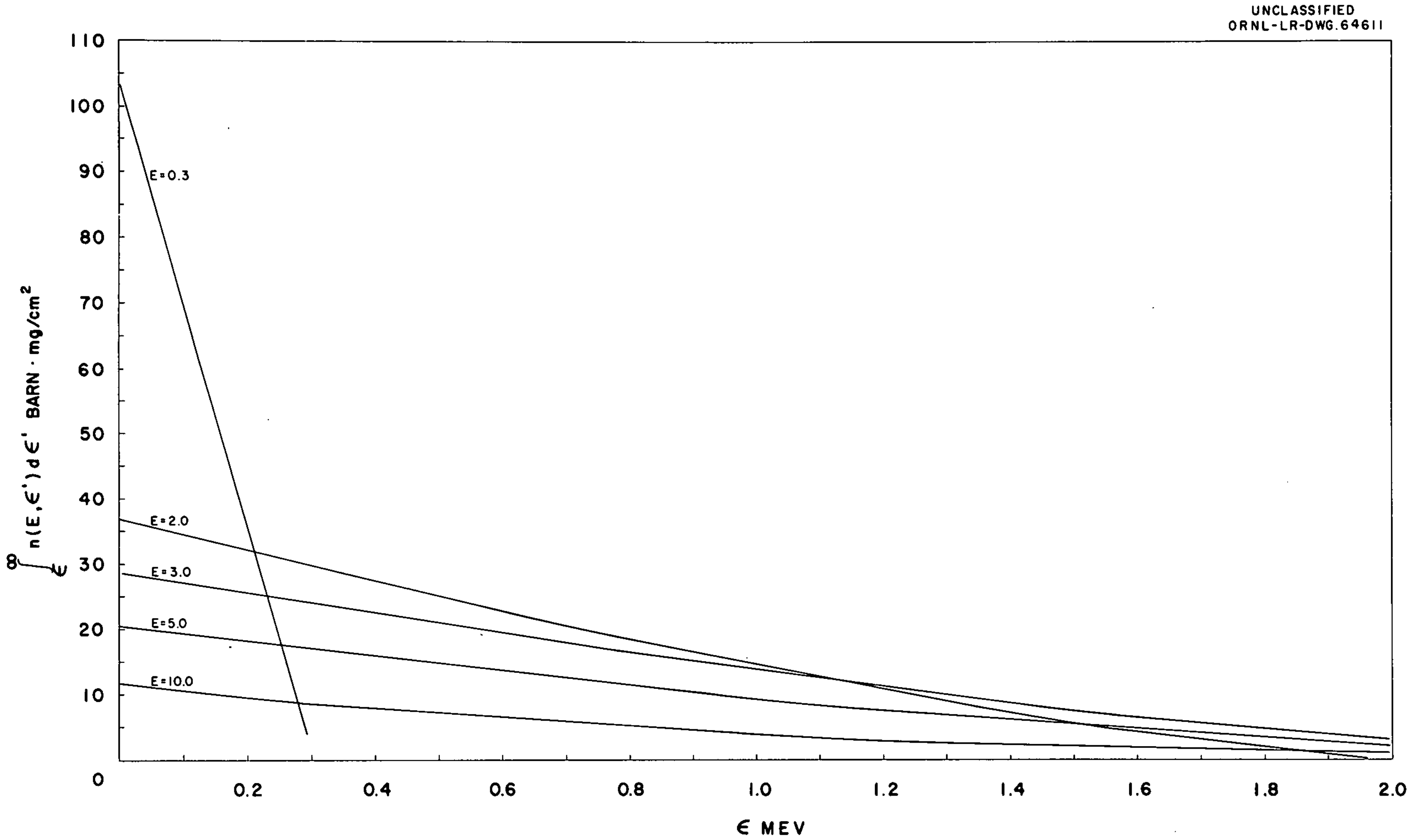

Fig. 4. Integral Response of Plane Detector, Normal Irradiation. (3.0 Mev gas, 0 Mev wall)

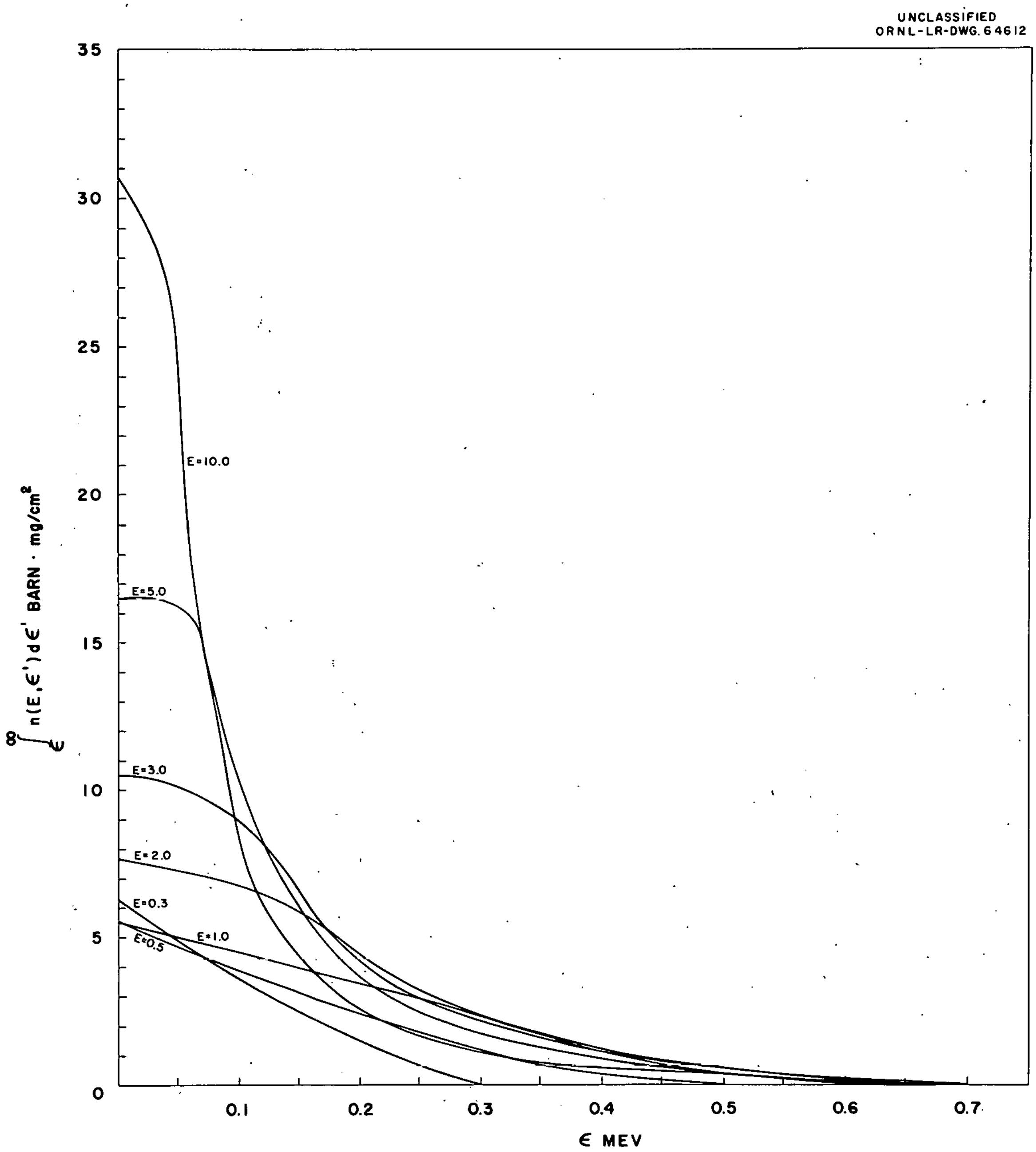

Fig. 5. Integral Response of Plane Detector, Normal Irradiation. (0.5 Mev gas, ∞ wall)

UNCLASSIFIED
ORNL-LR-DWG. 64613

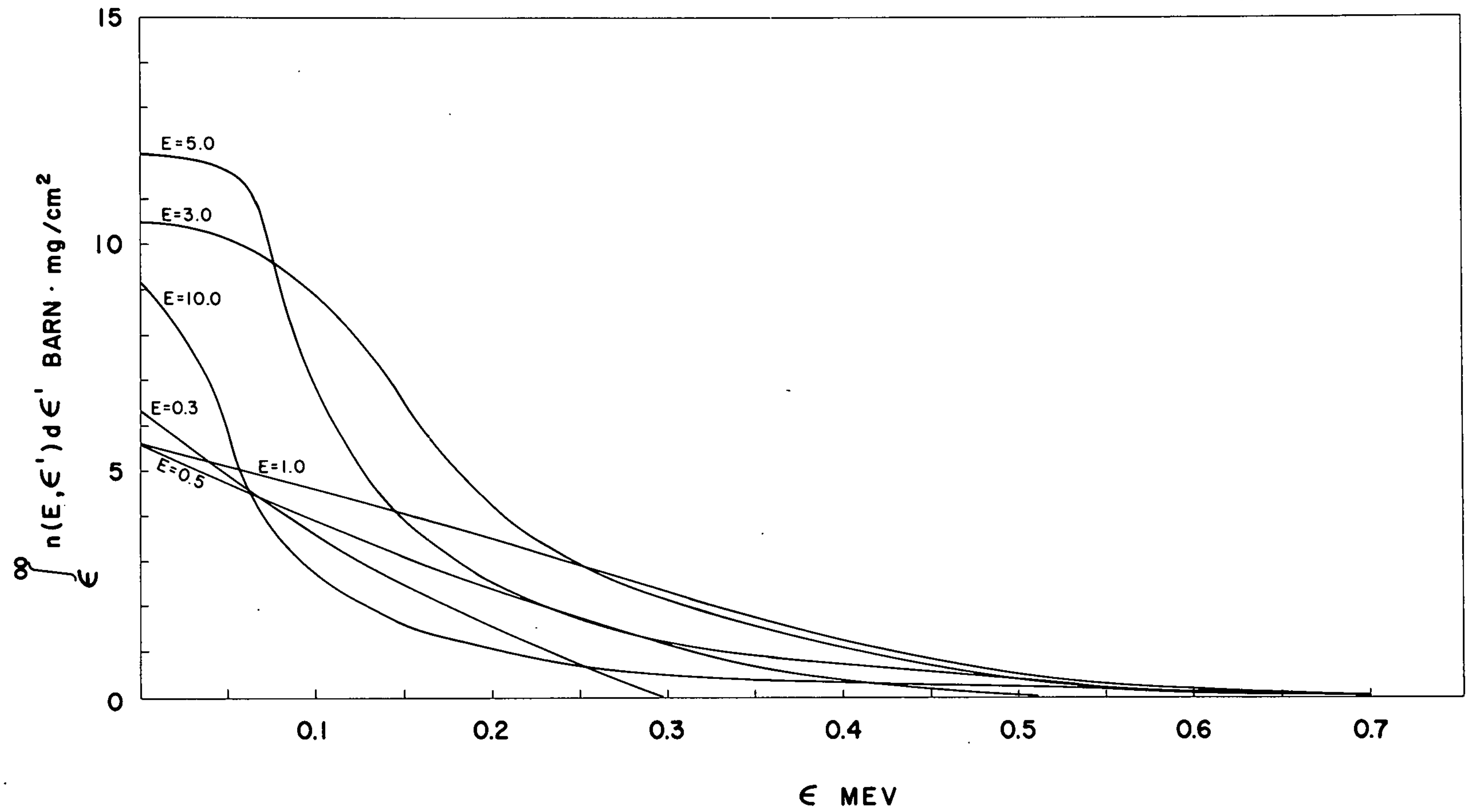

Fig. 6. Integral Response of Plane Detector, Normal Irradiation. (0.5 Mev gas, 3.0 Mev wall)

UNCLASSIFIED
ORNL-LR-DWG. 64614

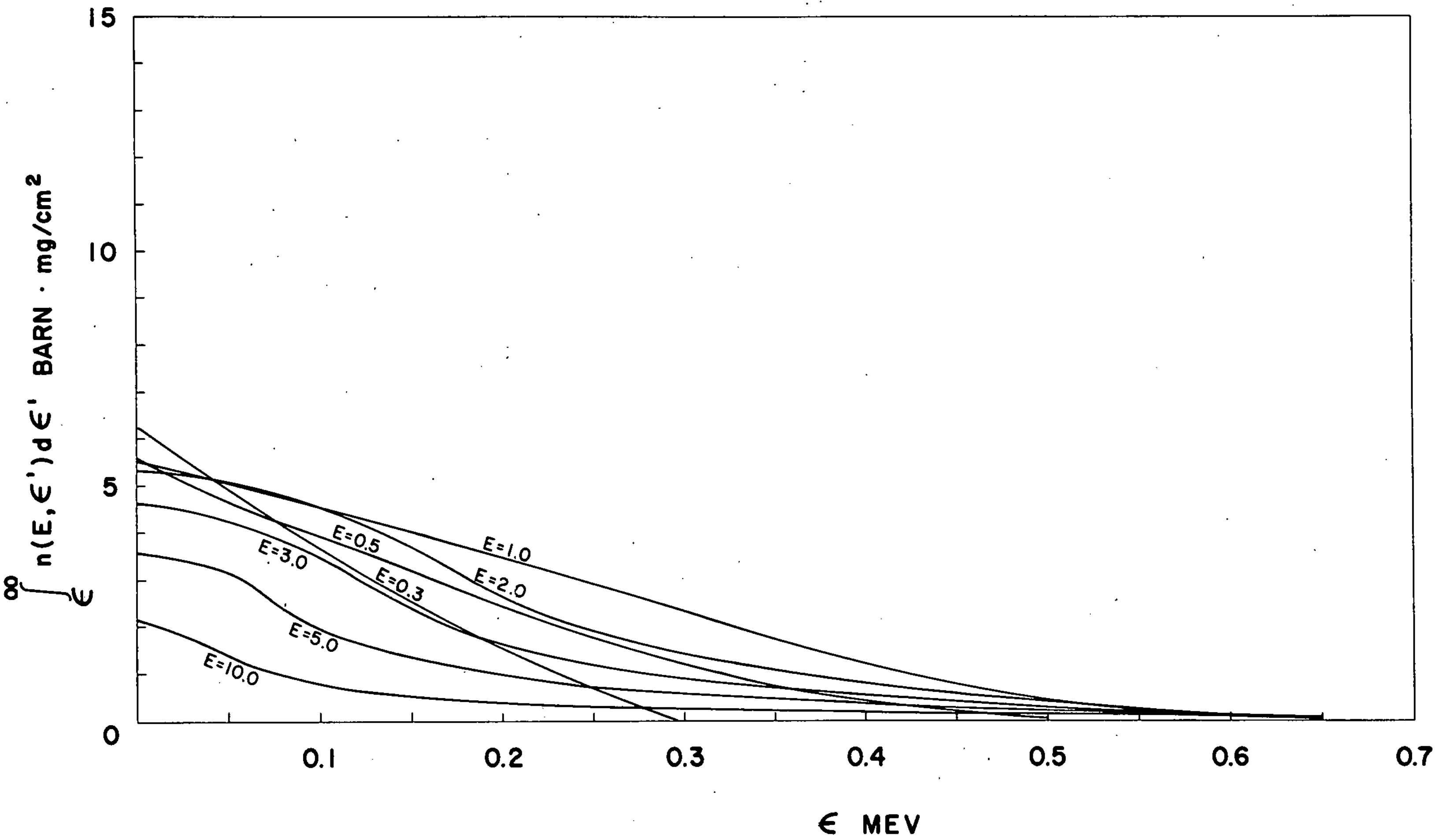

Fig. 7. Integral Response of Plane Detector, Normal Irradiation. (0.5 Mev gas, 1.0 Mev wall)

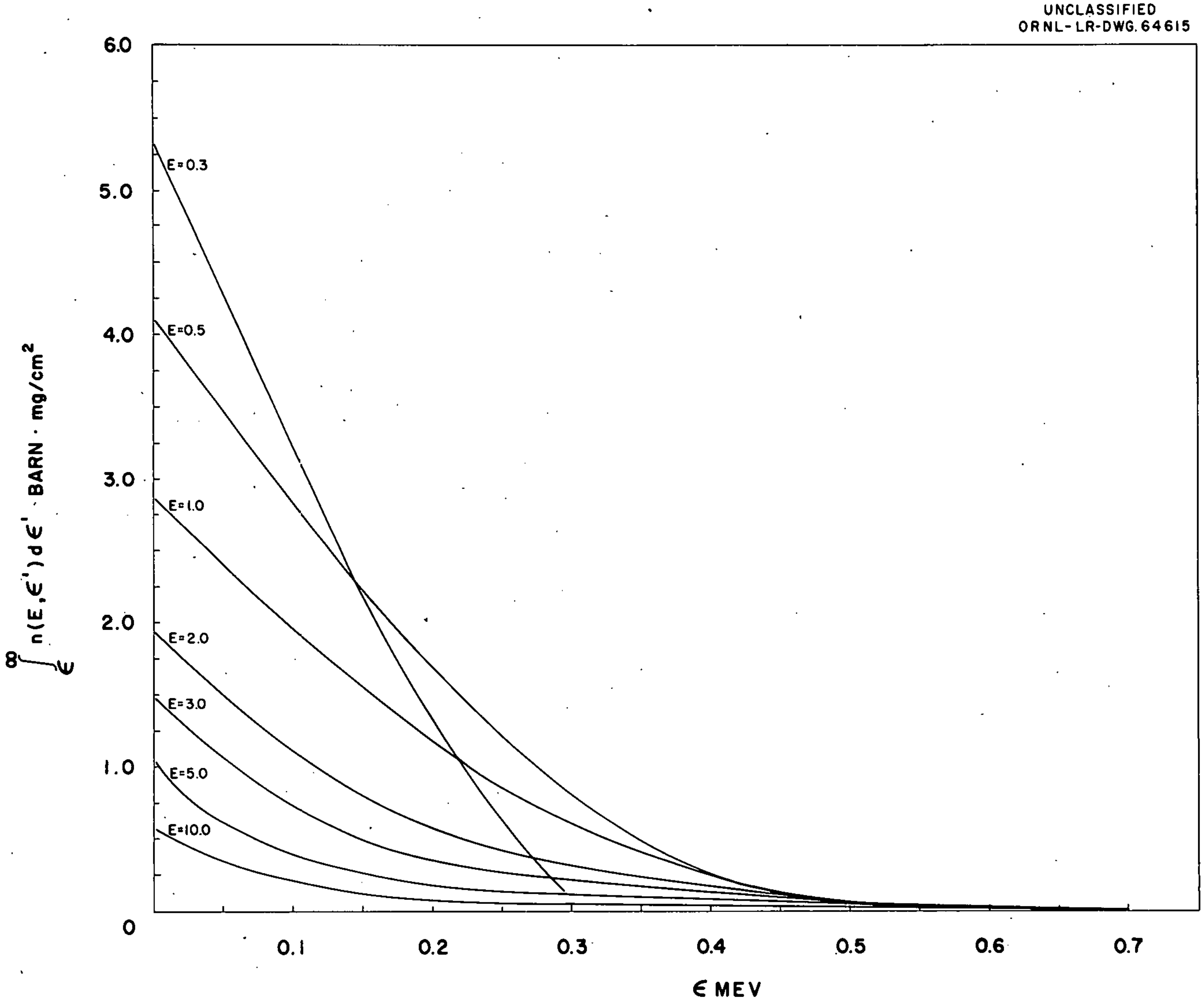

Fig. 8. Integral Response of Plane Detector, Normal Irradiation. (0.5 Mev gas, 0 Mev wall)

UNCLASSIFIED
ORNL-LR-DWG 64616

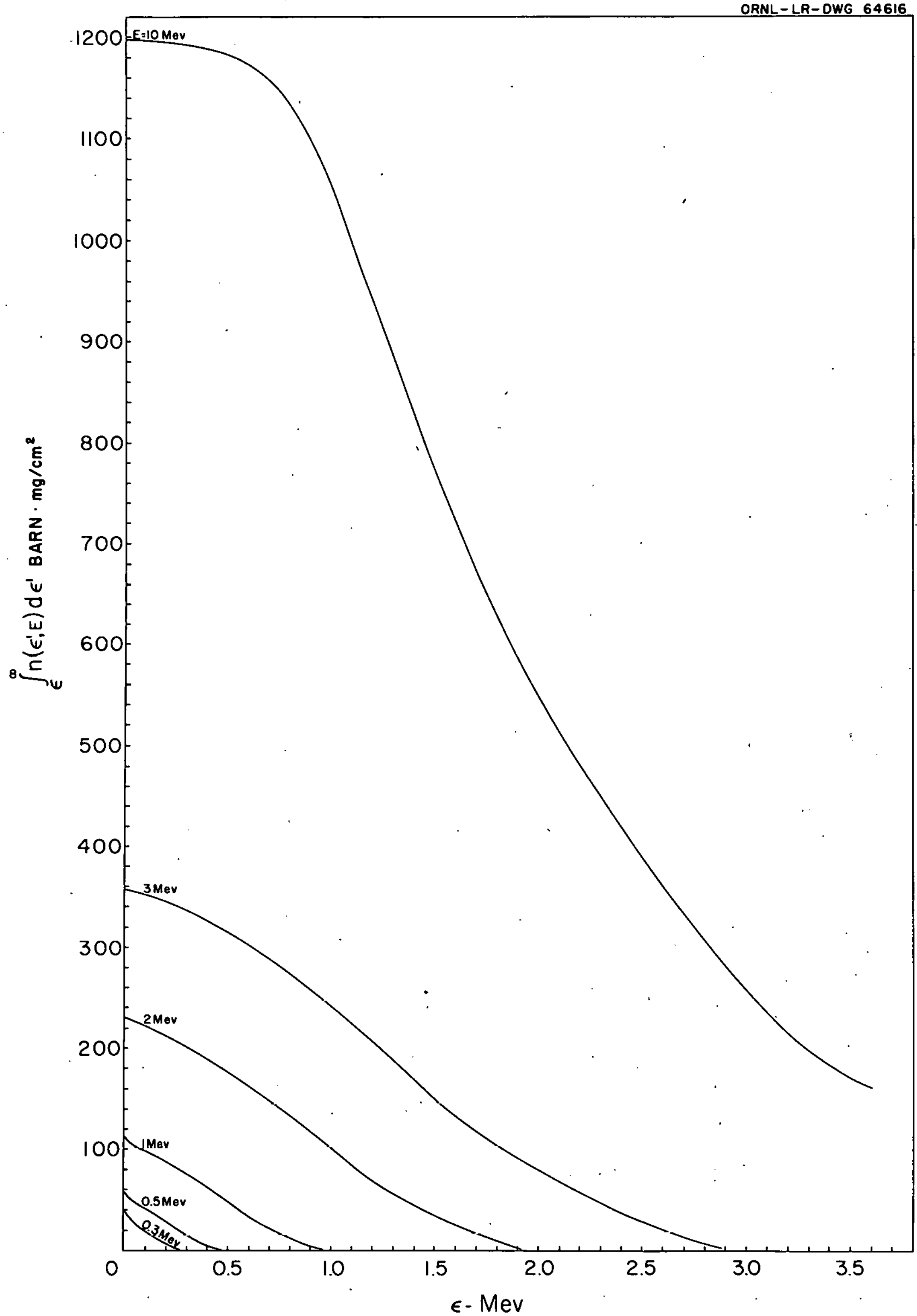

Fig. 9. Integral Response of Plane Detector, Isotropic Irradiation. (3 Mev gas, 10 Mev wall)

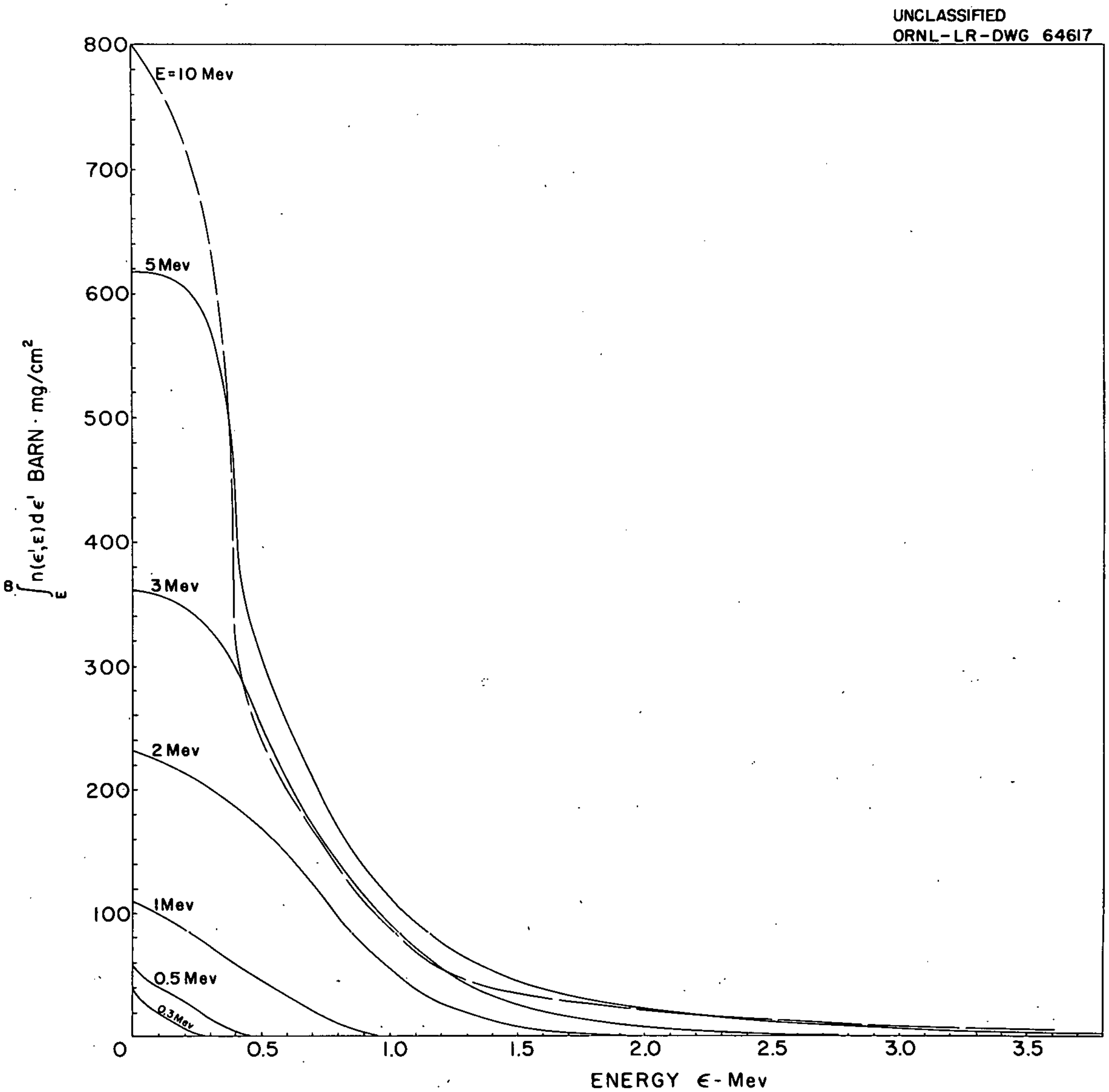

Fig. 10. Integral Response of Plane Detector, Isotropic Irradiation. (3 Mev gas, 5 Mev wall)

UNCLASSIFIED
ORNL-LR-DWG 64618

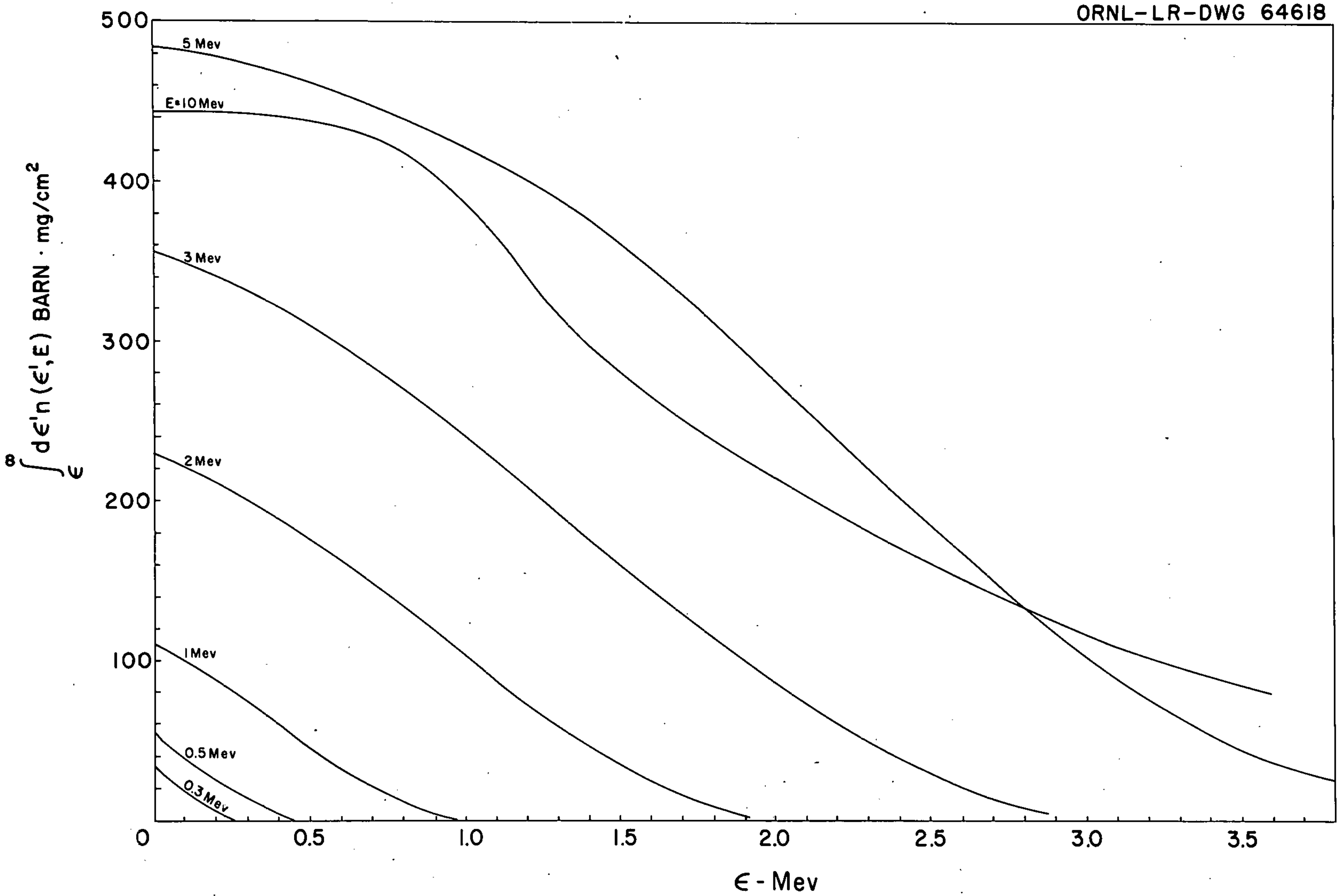

Fig. 11. Integral Response of Plane Detector, Isotropic Irradiation. (3 Mev gas, 3 Mev wall)

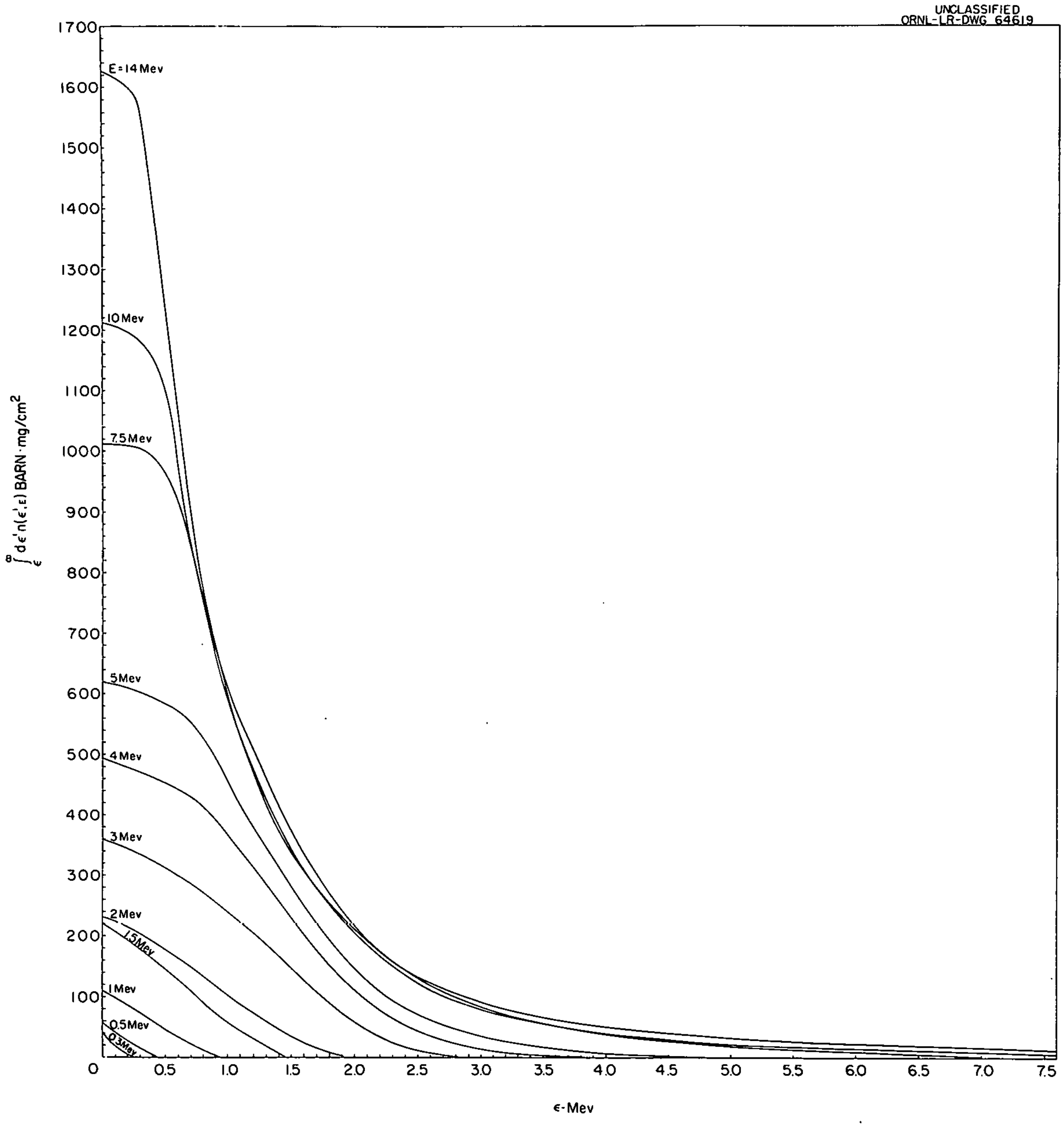

Fig. 12. Integral Response of Plane Detector, Isotropic Irradiation. (2 Mev gas, 14 Mev wall)

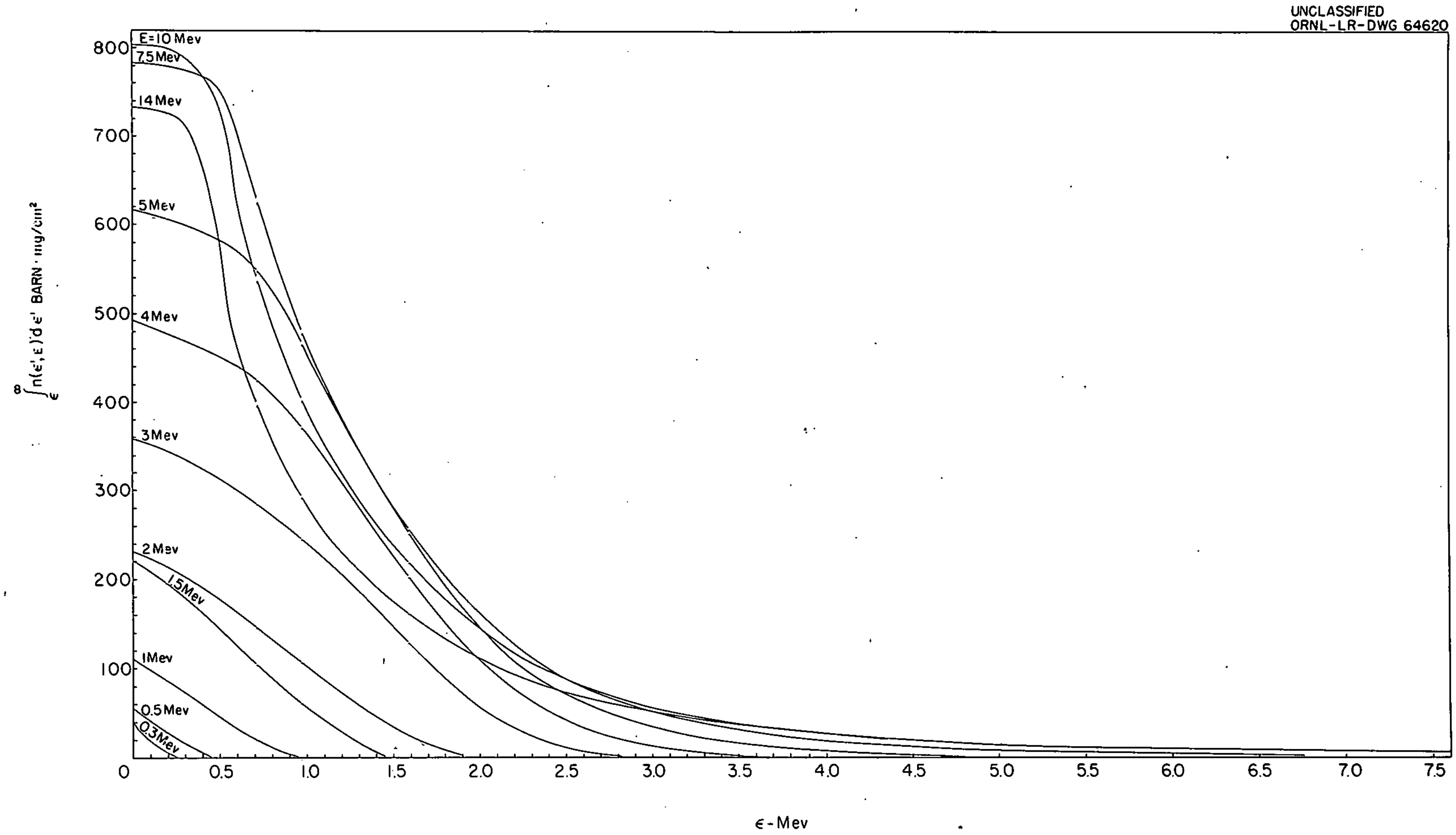

Fig. 13. Integral Response of Plane Detector, Isotropic Irradiation. (2 Mev gas, 5 Mev wall)

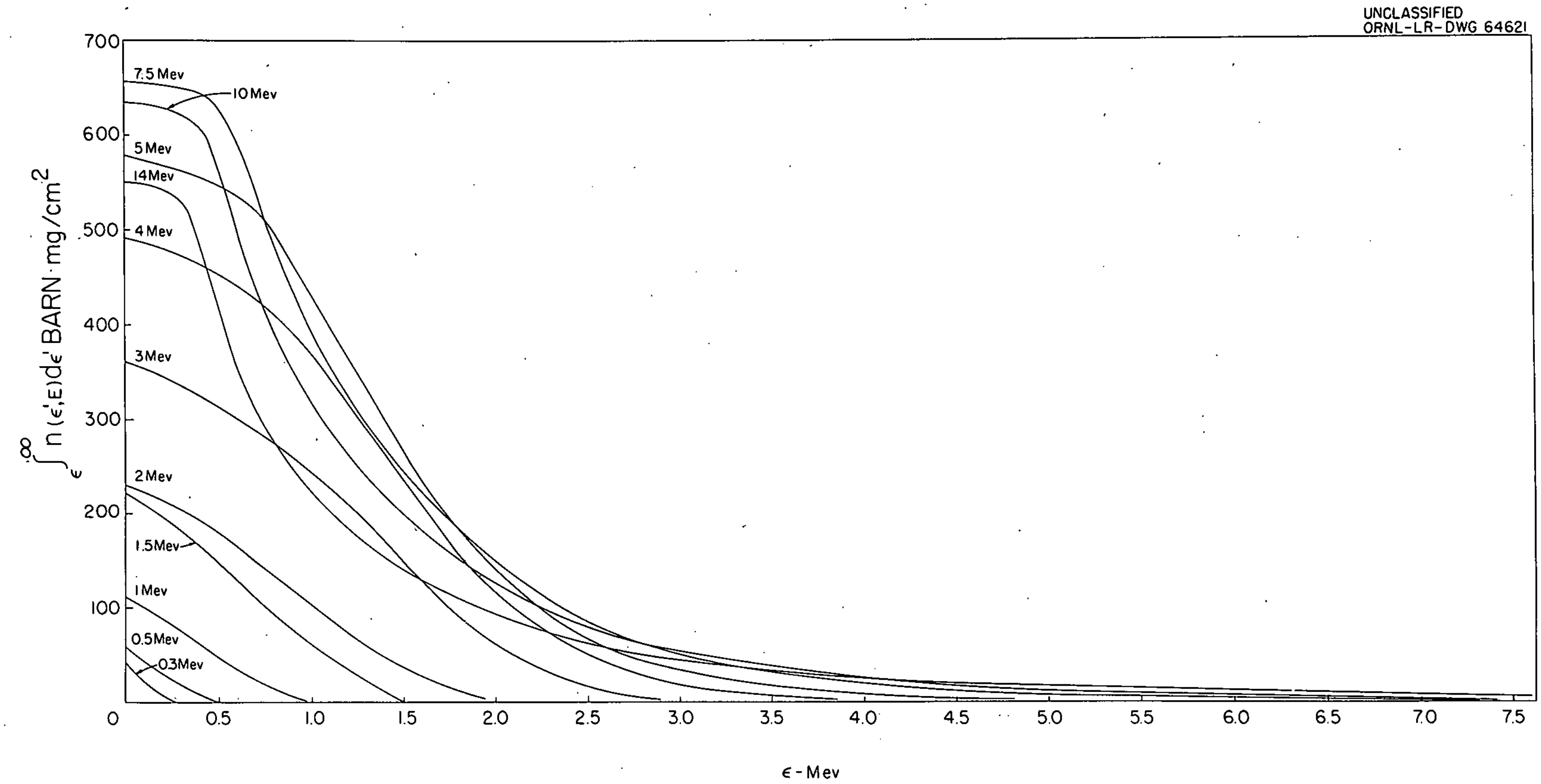

Fig. 14. Integral Response of Plane Detector, Isotropic Irradiation. (2 Mev gas, 4 Mev wall)

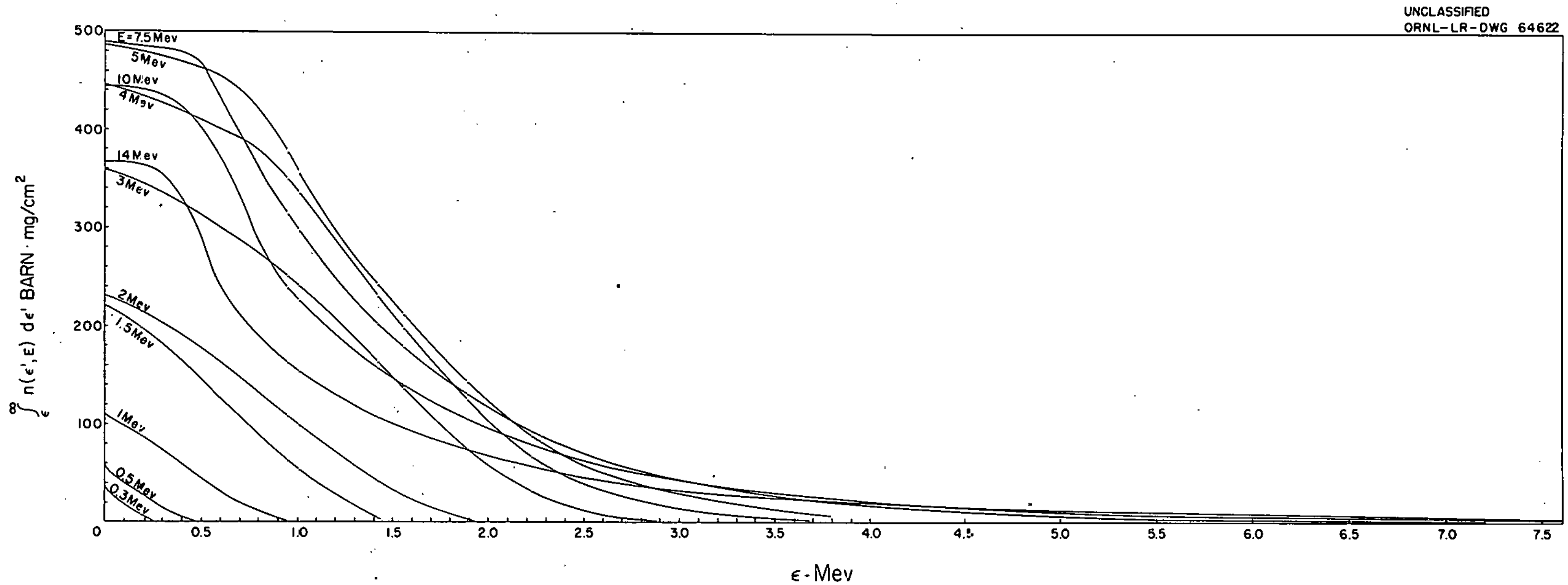

Fig. 15. Integral Response of Plane Detector, Isotropic Irradiation. (2 Mev gas, 3 Mev wall)

UNCLASSIFIED
ORNL-LR-DWG 64623

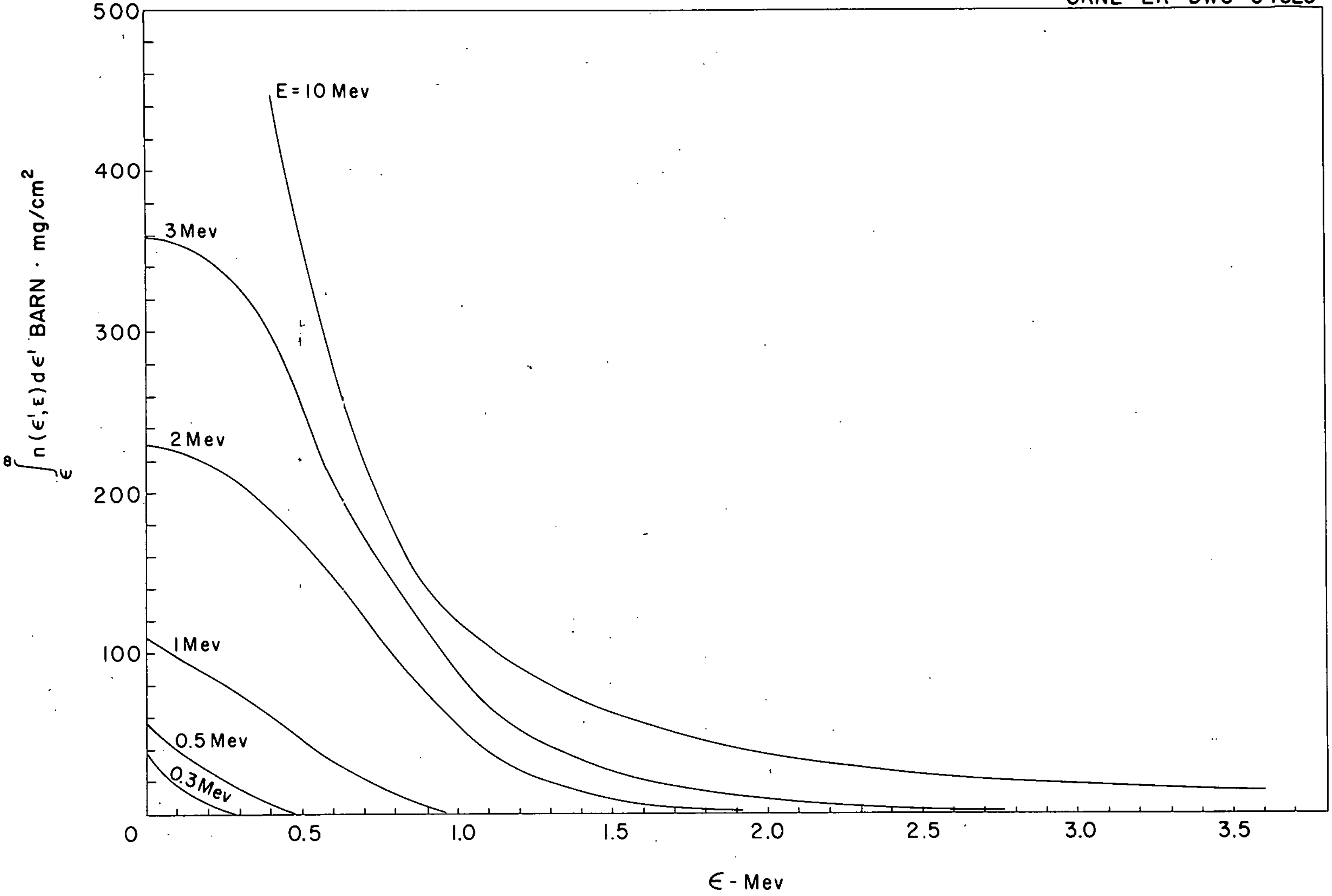

Fig. 16. Integral Response of Plane Detector, Isotropic Irradiation. (1 Mev gas, 10 Mev wall)

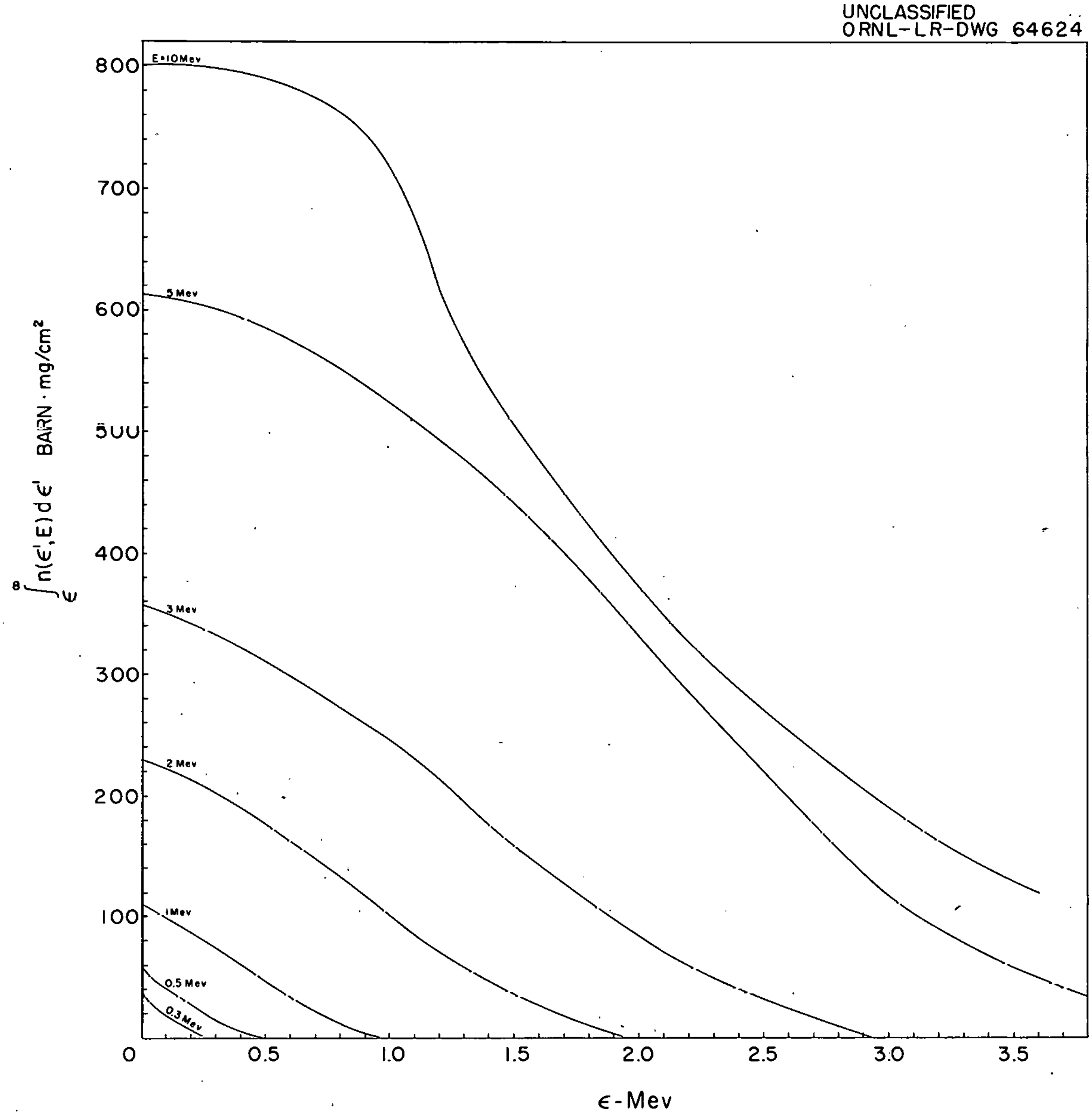

Fig. 17. Integral Response of Plane Detector, Isotropic Irradiation. (1 Mev gas, 5 Mev wall)

UNCLASSIFIED
ORNL-LR-DWG 64625

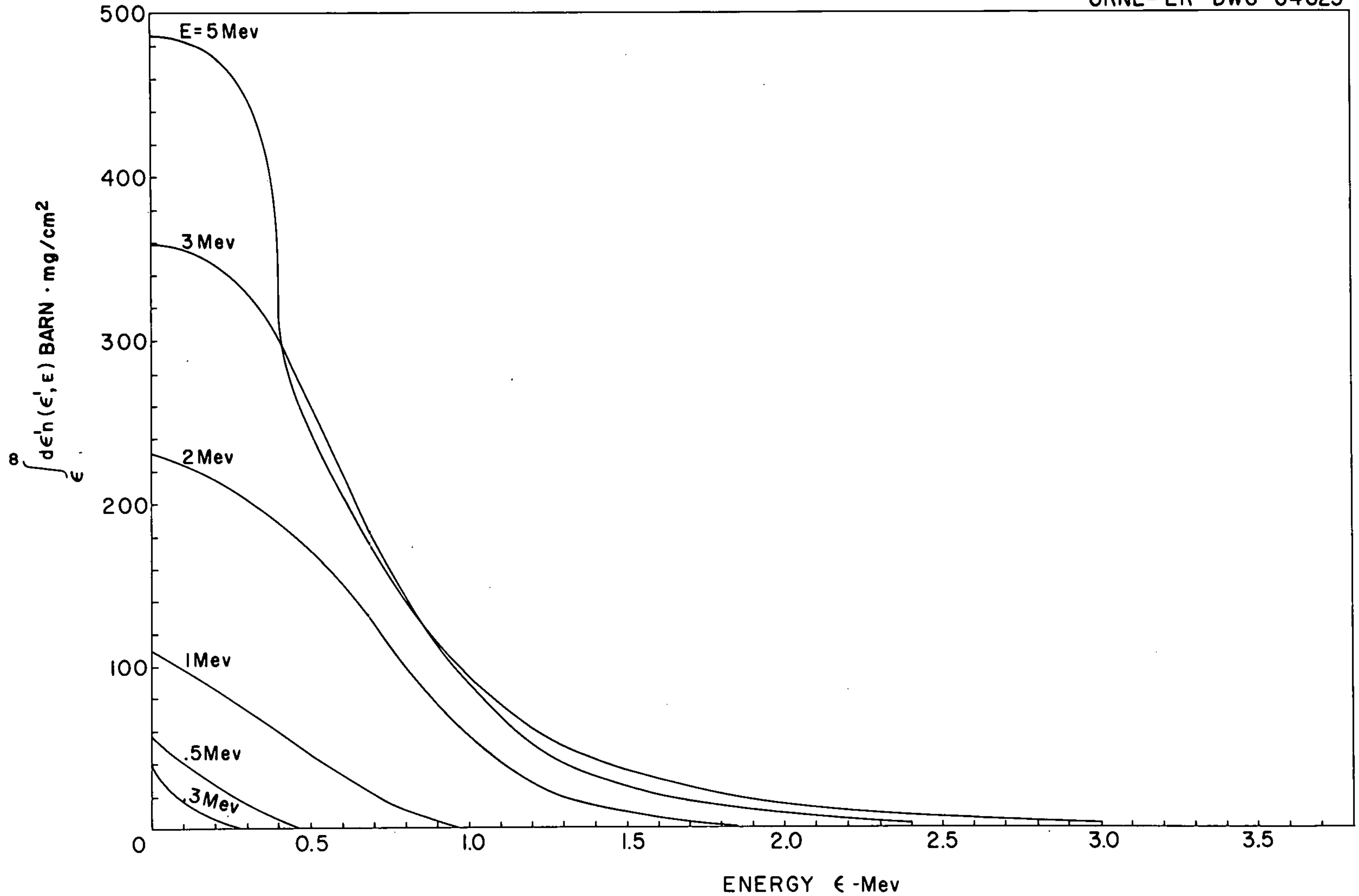

Fig. 18. Integral Response of Plane Detector, Isotropic Irradiation. (1 Mev gas, 3 Mev wall)

References

1. G. S. Hurst and R. H. Ritchie, Health Phys. 8, 117 (1962).
2. G. S. Hurst, R. H. Ritchie, and H. N. Wilson, Rev. Sci. Instr. 22, 981 (1951).
3. B. J. Moyer, Nucleonics 10, No. 5, 14 (1952); R. Skjoldebrand, J. Nuclear Energy 1, 299 (1955).
4. I. I. Petrov, Atomnya Energiya 3, 326 (1959).
5. R. H. Ritchie, Health Phys. 2, 73 (1958).
6. J. L. Hershfelder and J. L. Magee, Phys. Rev. 73, 207 (1948).
7. J. M. Blatt and V. F. Weisskopf, THEORETICAL NUCLEAR PHYSICS (John Wiley and Sons, New York, 1952) p 66.

THIS PAGE

WAS INTENTIONALLY

LEFT BLANK

ORNL-3089
UC-34 — Physics
TID-4500 (17th ed.)

INTERNAL DISTRIBUTION

1. Biology Library
2-3. Central Research Library
4. Reactor Division Library
5. Laboratory Shift Supervisor
6. ORNL — Y-12 Technical Library Document Reference Section
7-56. Laboratory Records Department
57. Laboratory Records, ORNL R.C.
58. R. G. Alsmiller
59. R. D. Birkhoff
60. J. C. Hart
61. G. S. Hurst
62. G. H. Jenks
63. R. G. Jordan (Y-12)
64. W. H. Jordan
65. C. E. Larson
66. K. Z. Morgan
67. J. P. Murray (K-25)
68-92. R. H. Ritchie
93. M. J. Skinner
94. J. A. Swartout
95. D. K. Trubey
96. A. M. Weinberg
97. C. D. Zerby
98. G. M. Fair (consultant)
99. J. C. Frye (consultant)
100. W. H. Langham (consultant)
101. E. P. Odum (consultant)
102. R. L. Platzman (consultant)
103. L. S. Taylor (consultant)

EXTERNAL DISTRIBUTION

104-108. H. B. Eldridge, Aerospace Corporation, 2400 El Segundo Blvd., El Segundo, California
109-113. P. R. Flusser, 616 S. Sycamore St., Ottawa, Kansas
114. Division of Research and Development, AEC, ORO
115-746. Given distribution as shown in TID-4500 (17th ed.) under Physics category (75 copies - OTS)